

# Polymer Chemistry

Accepted Manuscript



This is an *Accepted Manuscript*, which has been through the Royal Society of Chemistry peer review process and has been accepted for publication.

*Accepted Manuscripts* are published online shortly after acceptance, before technical editing, formatting and proof reading. Using this free service, authors can make their results available to the community, in citable form, before we publish the edited article. We will replace this *Accepted Manuscript* with the edited and formatted *Advance Article* as soon as it is available.

You can find more information about *Accepted Manuscripts* in the [Information for Authors](#).

Please note that technical editing may introduce minor changes to the text and/or graphics, which may alter content. The journal's standard [Terms & Conditions](#) and the [Ethical guidelines](#) still apply. In no event shall the Royal Society of Chemistry be held responsible for any errors or omissions in this *Accepted Manuscript* or any consequences arising from the use of any information it contains.

# Synthesis, Photophysical and Supramolecular Study of $\pi$ -Conjugated (diethylene glycol methyl ether) Benzoateethynylene Oligomers and Polymer

Cite this: DOI: 10.1039/x0xx00000x

Received 00th January 2012,  
Accepted 00th January 2012

DOI: 10.1039/x0xx00000x

www.rsc.org/

D. Meza,<sup>a</sup> E. Arias,<sup>\*a</sup> I. Moggio,<sup>a</sup> J. Romero,<sup>a</sup> J. M. Mata,<sup>a</sup> R. M. Jiménez-Barrera,<sup>a</sup> R. F. Ziolo,<sup>a</sup> O. Rodríguez,<sup>a</sup> M. Ottonelli<sup>b</sup>

We report on the synthesis of a trimer, pentamer, heptamer and a polymer of the (benzoate)ethynylene type bearing highly polar diethylene glycol methyl ethers as side chains. All of the materials were characterized by <sup>1</sup>H, DEPT-135, APT, <sup>13</sup>C NMR, UV-Vis, static and dynamic fluorescence spectroscopy. The X-ray scattering patterns of the pentamer and heptamer revealed a Smectic C lamellar order of the molecules, while the polymer was of the Nematic type, however any known texture reported in literature was observed by POM. The general term to classify the mesomorphic behaviour of these materials is Sanidic liquid crystals (LCs), which is consistent with their molecular shape assembly resembling bricks or board-like structures. The distance within the lamellae of 2.1, 2.3 and 2.0 nm for the pentamer, heptamer and polymer, respectively, is almost twice the distance of a single molecule in its more extended conformation of 1.48 nm. Therefore, the model of organization is consistent with a supramolecular assembly in bilayers, as was found in other (alkyl)benzoateethynylenes, where the side chains are oriented in the opposite sense, in a back-to-back "comb like" style. The strong  $\pi$ - $\pi$  interaction that governs these materials was evidenced by the repeated distance of 0.35 nm found by both X-ray scattering and HRTEM microscopy, which corresponds to the distance between conjugated chains. Photophysical properties are discussed as a function of the conjugation length and of the iodine or hydrogen terminal groups and are supported by theoretical calculations.

## INTRODUCTION

Phenyleneethynylenes (PPEs) are highly fluorescent conjugated molecules largely studied for their application as molecular markers and in optoelectronic devices, mainly light emitting diodes and biosensors. In this latter area, the construction of well-structured multilayered nano-films of PPEs by deposition techniques such as Langmuir-Blodgett (LB) or Layer-by-Layer (LBL) is of great importance, since devices can be developed where the last deposited layer could bear a biological or biomimetic receptor able to interact with specific analytes; the precedent layers can consist of either the same or other PPE macromolecules and can be used for signal detection and quantification by fluorescence. The devices may be constructed with the minimal amount of PPE material in a relatively small

area. The main features that PPEs should present, in order to be suitable for such application, are: 1) high fluorescence quantum yield; this should be as highest as possible because the analytes of interest in bio or chemical sensing are usually soluble in water and the dissolved oxygen in water dramatically quenches the emission, 2) to be amphiphilic or at least to present polar groups that could interact with the receptors to be deposited, which are usually soluble in water. Amphiphilicity is a very important feature for the LB film formation, since the fluorescent part must be transferred from the air-water interface to the substrate in a high order. The concept of sensor development based on PPEs LB or LBL films has been demonstrated by several works, for instance, by Swager's group<sup>1</sup> who pioneered this concept by reporting the use of PPE sensors for the detection of explosives, through quenching of

the fluorescence of the conjugated molecule. Actually, the quenching effect was attributed to an electron-transfer-mechanism in the thin films exposed to vapor specifically of 2,4,6-trinitrotoluene and 2,6-dinitrotoluene. We previously reported LBL films of a phenylethyne polymer where the last layer was a  $\beta$ -lactamase enzyme used for the fluorescent detection of gram negative antibiotics<sup>2</sup>. We also reported that benzoateethynylene oligomers bearing 11-undecanol as side chains were amphiphilic enough to form stable LB multilayers<sup>3</sup>, where the molecules were self-assembled in bilayers, with the –OH immersed in the water, and the –C<sub>11</sub>H<sub>22</sub>–, as well as the benzoates, were outside and perpendicular to the water surface and to the substrates when the films were transferred. In addition, we reported that the photoluminescence quantum yield in multilayer films increases as a function of the number of LB layers transferred to substrates up to 5 bilayers; the quantum yield of these assemblies drastically decreased with increasing numbers of layers, likely due to photon re-absorption. Despite that no biosensors were constructed in this previous work, the results suggested that biosensors could be constructed even with monomolecular layers. PPEs bearing glycol side chains are water soluble materials that can be used as molecular markers, which is also an area of great interest in the biology- and biotechnology-supramolecular chemistry field, i.e. folate-substituted PPE's is a fluorescent contrast agent to image cancer cells<sup>4</sup> or mannose-substituted PPE's<sup>5</sup> have been used for the recognition of the FimH expressed by the uropathogen *E.coli*. as molecular markers, the so contrasted cancer cells or bacteria can be characterized by spectroscopy or imaging techniques, by monitoring qualitatively and quantitatively their fluorescence, or by Confocal microscopy or even by Raman spectroscopy due to the vibrational sensitivity of the triple bond to lasers<sup>6</sup>, giving a net signal at around 2200 cm<sup>-1</sup>. However, the synthesis of PPEs substituted with glycol side chains represents a challenge since glycols tend to chelate the catalyst; moreover, the oxygen from the medium trapped in the glycols promotes the self-coupling of acetylenes to form butadiynes, giving rise to low yields of the target oligomers. In this work we report an oligomer series, Fig. 1: trimer **3BEgly-H**, pentamer **5BEgly-H** and heptamer **7BEgly-H** oligomers bearing highly polar diethylene glycol methyl ether as side chains, which can be obtained in good yields by the bi-directional iterative divergent-convergent approach. The homologue polymer, **I-nBEgly**, can also be synthesized by the Sonogashira reaction in good yields. Moreover, we report that incorporation of the glycols strongly increases the fluorescence quantum yield of the series with respect to other PPEs previously studied in our laboratory<sup>3a-b,7</sup> (under the same experimental conditions), with a maximal value for the quantum yield in solution of  $\phi = 0.70$  to  $0.97$  (depending on the solvent) for the pentamer by excitation at 310 nm. It was also found that these highly polar macromolecules self-assemble in bilayers in a typical “comb-like” fashion that are usually exhibited by other highly hydrophobic and/or amphiphilic benzoateethynylene macromolecules. From the SWAXS and HRTEM study, we conclude that the  $\pi$ - $\pi$  interaction that

governs in the benzoateethynylenes, gives rise first, to a self-assembly in bilayers, and then to a package of blocks of molecules resembling bricks. Because of their molecular shape and mesomorphic behavior, these materials were classified as Sanidic liquid crystals, a term that was used to classify other similar phenyleneethynylene materials<sup>7,8</sup>.

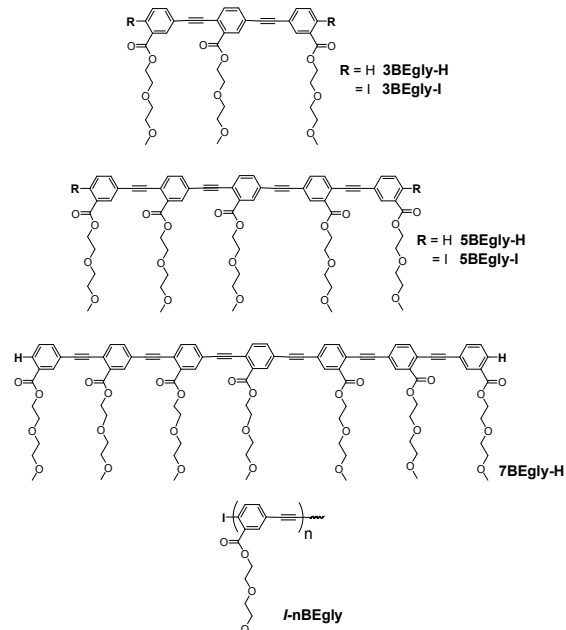


Fig.1. Chemical structure of (diethylen glycol methyl ether) benzoateethynylene oligomers and the homologue polymer.

## EXPERIMENTAL SECTION

### Equipment and methods.

<sup>1</sup>H and <sup>13</sup>C NMR data were obtained at room temperature with a Jeol Eclipse spectrometer at 300 MHz for <sup>1</sup>H and 75.4 MHz for <sup>13</sup>C using CDCl<sub>3</sub> as solvent and internal reference. The molecular weights were determined by GPC on an HP 1100 HPLC using PS standards and refractive index as detector. A series of three HP PLGel columns were used: 10<sup>3</sup>, 10<sup>5</sup> and 10<sup>6</sup> Å and THF as the mobile phase at 40 °C and 1 mL/min. Thermogravimetric (TGA) and differential scanning calorimetry (DSC) analyses were carried out on a DuPont 951 instrument under nitrogen at a heating rate of 10 °C/min. Small and wide angle X ray scattering patterns were obtained with a Anton Paar SAXSess mc<sup>2</sup> SWAXS instrument using CuK $\alpha$  radiation at a wavelength of 0.1542 nm. UV-Vis spectra were recorded on an Agilent 8453 spectrophotometer. Fluorescence spectra were carried out on a Perkin Elmer LS50B spectrofluorimeter with a circulating water bath at 25.0  $\pm$  0.3°C. Excitation wavelength was 310 nm. Fluorescence quantum yields were obtained according to the literature and using as standard 0.1N H<sub>2</sub>SO<sub>4</sub> solution, Harmane ( $\phi=0.82$ )<sup>9</sup>. Three different samples with optical density at 310 nm between 0.05 and 0.1 were analysed and the average value was reported as  $\phi_F$ . Fluorescence lifetimes were obtained using the Time Correlated Single Photon Counting technique (TCSPC) with a

TemPro (Horiba Scientific) instrument. A nanoLED laser at 295 nm was used for the excitation; the probe measurement was obtained with a 0.01% ultrapure water suspension of LUDOX (Aldrich). Calibration of the equipment was realized with a POPOP [1,4-bis(4-methyl-5-fenil-2-oxazolyl)benzene] methanol solution (optical density <0.1 and lifetime of 0.93ns).[10] Data were fit with the DAS6 software available with the equipment.

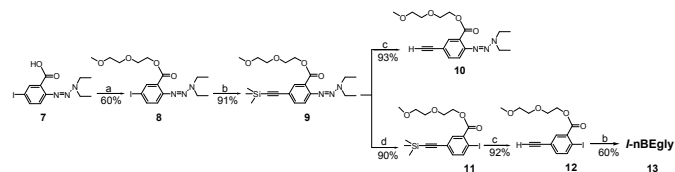
### Synthesis.

Experimental procedures, chemical and physicochemical characterization of each compound are given in the electronic supplementary Information (ESI) section. Reactions were carried out at the local ambient pressure of 84.5 kPa.

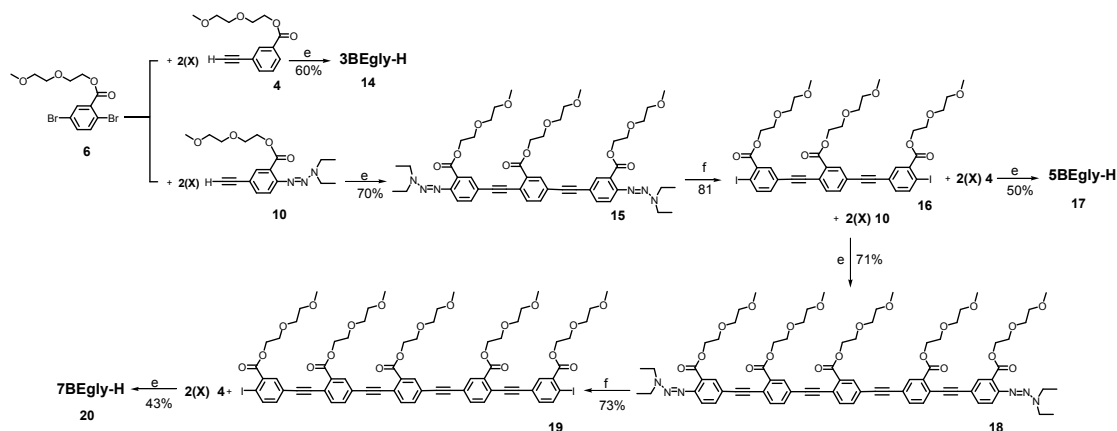
## RESULTS AND DISCUSSION

### Syntheses.

In the preparation, the oligomers were obtained in odd numbers by applying a bi-directional convergent-divergent strategy that we recently reported<sup>7</sup> and that is mainly based in the preparation of a triazene-trimethylsilylethynyl monomer **10**, Scheme 1. In addition, monomer **6** was used as the core for the bidimensional synthesis, while monomer **4** was used to obtain hydrogen terminated oligomers, Scheme 1S.



**Scheme 1** Reagents and conditions: (a) diethylene glycol methyl ether, DCC/DMAP, CH<sub>2</sub>Cl<sub>2</sub>, 0 °C, 15h; (b) TMSA, [(C<sub>6</sub>H<sub>5</sub>)<sub>3</sub>P]<sub>2</sub>PdCl<sub>2</sub> (5.0 % mol), CuI (1.5 % mol), Et<sub>3</sub>N, DMF, 80 °C, 16h; (c) TBAF, THF, rt, 12 min.; (d) CH<sub>3</sub>I, 120 °C, vacuum, 15h.



**Scheme 2** Reagents and conditions: (e) [(C<sub>6</sub>H<sub>5</sub>)<sub>3</sub>P]<sub>2</sub>PdCl<sub>2</sub> (5.0 % mol), CuI (1.5 % mol), Et<sub>3</sub>N, DMF, 80 °C, 16h.; (f) CH<sub>3</sub>I, 120°C, vacuum, 15h.

Glycolic chains imparted a polar and amphiphilic character to the materials and were introduced by a condensation reaction between the carboxylic acids: 2-(3,3-diethyltriazene)-5-iodo benzoic acid **7**, 3-iodo benzoic acid **1** and 2,5-dibromo benzoic acid **5** with the diethylene glycol methyl ether under *N,N'*-dicyclohexylcarbodiimide (DCC)/DMAP-mediated esterification conditions in CH<sub>2</sub>Cl<sub>2</sub>. In a first step, Scheme 2, trimer **3BEgLy-H** was obtained in 60 % yield by Pd/CuI cross-coupling two equivalents (eq.) of **6** with 2.2 eq. of **4**. For the synthesis of longer oligomers, the iterative

divergent/convergent synthesis started with the Pd/CuI cross-coupling of 1 eq. of **6** with 2.2 eq. of **10** to afford a triazene terminated trimer **15** in 70 % yield, from which the triazenes are substituted by iodine groups by heating **15** at 120 °C in CH<sub>3</sub>I in a vacuum sealed capsule for 15 h. The iodine terminated trimer **16** is the essential building core for the elongation of **nBEgLy** chains and must be obtained in large enough amounts. Therefore, **16** is divided in two portions, one portion undergoes Pd/CuI cross-coupling with 2 eq. of **4** to afford the pentamer **5BEgLy-H** in 50 % yield.

**Table 1.** Optical properties of the macromolecules studied in this work in different solvents.

Molecule	CH <sub>2</sub> Cl <sub>2</sub>				THF				Toluene			
	λ <sub>Abs</sub> (nm)	ε x 10 <sup>4</sup> (M <sup>-1</sup> cm <sup>-1</sup> )	λ <sub>Em</sub> (nm)	E <sub>S10</sub> (eV)	λ <sub>Abs</sub> (nm)	ε x 10 <sup>4</sup> (M <sup>-1</sup> cm <sup>-1</sup> )	λ <sub>Em</sub> (nm)	E <sub>S10</sub> (eV)	λ <sub>Abs</sub> (nm)	ε x 10 <sup>4</sup> (M <sup>-1</sup> cm <sup>-1</sup> )	λ <sub>Em</sub> (nm)	E <sub>S10</sub> (eV)
<b>3BEgLy-H (14)</b>	335	4.0	369	3.4	333	4.68	366	3.4	335	4.11	368	3.4
<b>3BEgLy-I (16)</b>	343	8.41	376	3.3	342	9.20	375	3.3	345	8.32	378	3.3
<b>5BEgLy-H (17)</b>	367	11.62	402	3.1	365	136.6	400	3.3	368	13.11	403	3.1
<b>5BEgLy-I (19)</b>	368	12.40	405	3.1	368	13.20	404	3.3	369	12.20	407	3.1
<b>7BEgLy-H (20)</b>	372	12.96	414	3.0	372	14.52	412	3.3	375	14.16	415	3.0
<b>I-nBEgLy (13)</b>	375	9.22	423	3.0	376	10.11	421	3.0	378	9.5	424	3.0

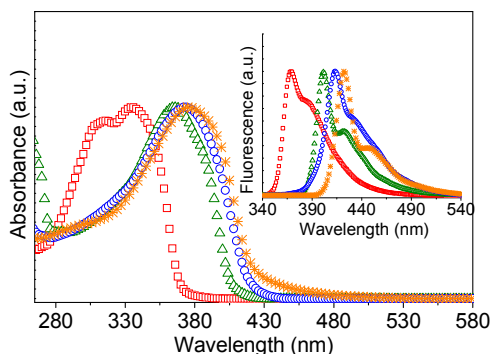


Fig. 2 UV-Vis and (inserted) fluorescence spectra in  $\text{CH}_2\text{Cl}_2$  of **3BEgly-H** (■), **5BEgly-H** (●), **7BEgly-H** (▲) and **I-nBEgly** (★).

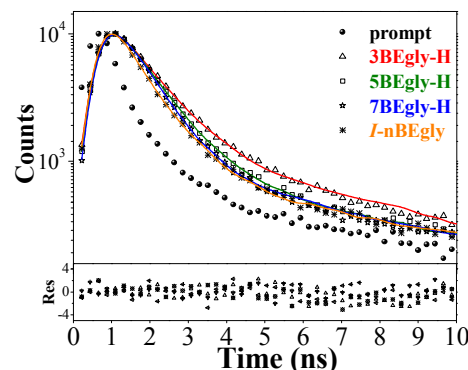


Fig. 3 Time Correlated Single Photon Counting technique (TCSPC) data for the series of macromolecules studied in this work in  $\text{CH}_2\text{Cl}_2$ .

The other portion of **16** is cross-coupled with 2.2 eq. of **10** to form the triazenes terminated pentamer **18**, which after their conversions to iodines, the pentamer **19** is obtained in 73 % yield. At this point and following these repetitive cycles of reactions, oligomers can be grown in odd numbers, however, and according to our experience, the effective conjugation can almost be attained for a heptamer, since a difference of ca. 10 nm of its maximum absorption wavelength is reached with respect to the homologue polymer<sup>3a,11</sup>. Thus, the heptamer **7BEgly-H** was obtained in 43 % yield by Pd/CuI cross-coupling **19** with **4**. It is worth mentioning that all of the oligomers were washed with a dithiocarbamate sodium salt solution in order to eliminate any remaining catalyst that could be complexed into the glycolic chains, and then purified by silica gel chromatography, and finally passed through gravimetric GPC column (Biorads, Bio-Beds SX1, toluene). In addition to the aforementioned oligomers, we synthesized the homologue polymer **I-nBEgly 13** by reacting (diethylene glycol methyl ether) 5-ethynyl-2-iodobenzoate **12**, Scheme 1, under the Sonogashira cross-coupling conditions, using  $\text{Et}_3\text{N}$  as solvent. When the polymerization reaction was stopped, the ammonium salt was filtered off and the solvent evaporated; the crude polymer was then re-solubilized in toluene and directly passed through gravimetric GPC column. The calculated average molecular weight ( $M_w$ ), numerical ( $M_n$ ), and the polydispersity index (PI) using PS standards are  $M_w = 8594$ ,  $M_n = 4316$ ,  $\text{PI} = 1.99$ . All of the macromolecules are soluble in  $\text{CH}_2\text{Cl}_2$ ,  $\text{CHCl}_3$ , THF, toluene, methanol, acetone and DMSO. Whereas **3BEgly-H** is a honey-like viscous liquid, **5BEgly-H**, **7BEgly-H** and **I-nBEgly** are green pasty materials. It is worth noting that **5BEgly-H** is a highly fluorescent green powder.

### The spectroscopic and photophysical properties

The spectroscopic and photophysical properties of the oligomers in different solvents are summarized in Tables 1 and 2. Fig. 2 shows the absorption and fluorescence (insert)

spectra of the **nBEgly** series in  $\text{CH}_2\text{Cl}_2$ . The absorption spectra of the oligomers are independent of the concentration discarding any ground state interactions (see supporting information)<sup>12</sup>. The main absorption peak  $\lambda_{\text{abs}}$  ascribed to the HOMO-LUMO electronic transition is observed between 335 and 372 nm with a bathochromic shift along the series according to the increase in the conjugation length<sup>13</sup>. The molar absorption coefficient  $\epsilon$  increases also as the number of chromophores increases. The fluorescence spectra are more resolved with respect to the absorption spectra presenting typical excitonic features. We note that the absorption and emission maxima of this series are very similar to those reported for a (cholesteryl) benzoateethynylene series, which indicates that the conjugation is mainly due to the benzoateethynylene backbone with no relevant effect of the substituent<sup>7</sup>. The emission spectra do not change with the excitation wavelength. Moreover, the excitation and absorption spectra are identical, thus revealing the existence of just one emitting state (see supporting information). In general, neither the absorption nor emission spectra change with solvents between  $\text{CH}_2\text{Cl}_2$ , THF and toluene, indicating that there is no-solvatochromism. The fluorescence quantum yield  $\phi$  is medium-high with a maximum value for the pentamer. This indicates that non radiative processes are occurring, with internal conversion being the most probable. Actually, the Stokes's shift  $\Delta\nu$  is in the same range of those molecules that pass from an "aromatic" to a more planar "quinoid" geometry after excitation<sup>14</sup> and interestingly, the trend in  $\Delta\nu$  is opposite to that of  $\phi$ , having the minimum value for the **5BEgly-H**. Intersystem crossing to a non-fluorescent triplet state cannot be discarded, as found for other phenyleneethynylenes<sup>3-5</sup>. This is more evident when the  $\phi$  values of the iodine substituted



**Table 2** Photophysical properties of the macromolecules studied in this work in different solvents.

Molecule	CH <sub>2</sub> Cl <sub>2</sub>					THF					Toluene				
	$\phi$ (%)	$\tau$ (ns)	$K_{\text{rad}}$ (ns <sup>-1</sup> )	$K_{\text{nr}}$ (ns <sup>-1</sup> )	$\Delta\nu$ (cm <sup>-1</sup> )	$\phi$ (%)	$\tau$ (ns)	$K_{\text{ad}}$ (ns <sup>-1</sup> )	$K_{\text{nr}}$ (ns <sup>-1</sup> )	$\Delta\nu$ (cm <sup>-1</sup> )	$\phi$ (%)	$\tau$ (ns)	$K_{\text{rad}}$ (ns <sup>-1</sup> )	$K_{\text{nr}}$ (ns <sup>-1</sup> )	$\Delta\nu$ (cm <sup>-1</sup> )
<b>3BEgly-H (14)</b>	45	0.61	0.74	0.33	2750	43	0.51	0.84	1.18	2708	47	0.64	0.73	0.83	2677
<b>3BEgly-I (16)</b>	7	0.24	0.29	3.87	2559	6	0.22	0.03	4.27	2573	7	0.22	0.32	4.23	2530
<b>5BEgly-H (17)</b>	82	0.39	2.10	0.46	2372	97	0.43	2.26	0.07	2397	70	0.25	2.80	1.20	2360
<b>5BEgly-I (19)</b>	48	0.20	2.40	2.60	2483	38	0.18	2.11	3.44	2421	31	0.25	1.24	2.76	2530
<b>7BEgly-H (20)</b>	48	0.26	1.85	2.0	2727	64	0.32	2.00	1.11	2610	43	0.17	2.53	3.35	2570
<b>I-nBEgly (13)</b>	40	0.14	2.86	4.29	3026	41	0.09	4.56	6.56	2843	39	0.15	2.60	4.01	2870

oligomers **3BEgly-I** and **5BEgly-I** are compared with those of the H substituted ones. A marked decrease is found even for the trimer **3BEgly-I** for which the Stokes' shift is lower. It is known that heavy atoms such as halogens favour intersystem crossing by lowering the energy of the triplet state<sup>15</sup>. This result could suggest that even in the H terminated oligomers, intersystem crossing is indeed responsible for the deviation from unity, which is confirmed by the lifetime measurements. Fig. 3 shows the TCSPC data for all the series. All of the TCSPC data for all oligomers were fitted with a three exponential curve. From the average lifetime  $\tau$ , the radiative and non-radiative constants were obtained. The H terminated pentamer presents the larger radiative and lower non radiative constants consistent with the higher quantum yield. Finally, we note importantly that the  $\phi$  values were obtained by exciting at 310 nm as for this pentamer, the quantum yield was higher than 1 if excited at 10 nm below the main absorption peak, as is usually done in our laboratory. Under these excitation conditions, the diethylene glycol methylether series **nBEgly** is, in general, more fluorescent than (11-undecanol) benzoateethynylene<sup>3a</sup> and (cholesteryl) benzoateethynylenes<sup>5,7</sup>. The lower values found for (cholesteryl) benzoateethynylenes that present the same conjugated backbone (and as previously discussed, similar absorption and emission maxima) can be explained on the basis of the quenching effect of the cholesteryl side chains as demonstrated in the ref.<sup>8</sup>, from the comparison between the

**Table 3.** TD-B3LYP/6-311G\*\* singlet and triplet excitation energies (nm) and corresponding oscillator strengths ( $f$ ) for **3BEgly-H** and **5BEgly-H** geometries depicted in Fig. 4.

<b>3BEgly-H (14)</b>		<b>5BEgly-H (17)</b>	
Singlet	Triplet	Singlet	Triplet
379.02 (1.40)	555.09	443.13 (3.15)	618.16
331.45 (0.11)	425.13	379.72 (0.02)	538.83
323.80 (0.00)	378.39	368.17 (0.01)	458.61
320.78 (0.02)	362.79	340.88 (0.02)	392.06

cholesteryl heptamer and (11-undecanol) benzoateethynylene (labelled **oPE7** in that paper). If we compare **oPE7** with **7BEgly-H**, the Stokes' shift is larger for the diethylene glycol methyl ether oligomer indicating that internal conversion losses are more important and that the quantum yield should be lower and not higher. However, the extinction coefficient is much larger and that could favour the enhancement of the fluorescence.

#### Theoretical calculations.

The quantum chemical calculations of the excited states were carried out in order to better understand the photophysical properties of the series. The Time-Dependent Density Functional Theory (TDDFT) approach was applied to the trimer **3BEgly-H** and pentamer **5BEgly-H**, by using the B3LYP functional with the 6-311G\*\* basis set. In order to save computational time, the glycolic side chains were retired and instead, methyl benzoate groups were considered; that is an approximation usually carried out by many authors as the side chains should not directly affect the nature of the electronic excitations<sup>12,13,16</sup>. However, the effect of the glycol chains in the geometry of the ground state was considered as the molecules were first obtained at AM1 level, without any constraint or approximation. Fig. 4a shows the lowest energetically (favored) conformation of **3BEgly-H**, where it is worth noting that benzoate moieties are not totally co-planar, having dihedral angles of 24° and 3° degree, respectively. This

**Table 4.** TD-B3LYP/6-311G\*\* singlet and triplet excitation energies (nm) and corresponding oscillator strengths ( $f$ ) for **3BEgly-H** and **5BEgly-H** geometries depicted in Fig. 5.

<b>3BEgly-H [90°,45°]</b>		<b>5BEgly-H [60°, 60°, 90°, 60°]</b>	
Singlet	Triplet	Singlet	Triplet
345.82 (0.69)	490.97	399.21 (0.00)	496.53
333.40 (0.20)	396.67	381.72 (1.42)	486.01
321.18 (0.02)	389.02	373.51 (0.48)	456.00
316.86 (0.00)	343.77	360.37 (0.15)	401.60

**Table 5.** Experimental calculated diffraction spacing  $d_{(100)}$  at a given  $2\theta$  angle for the molecules studied in this work,  $h$  is the corresponding theoretical molecular length of a bilayer on its more extended conformation,  $L$  is the conjugated backbone length found by X-ray, while  $L$  is the theoretical length of the benzoateethynylene backbone. The molecular tilt angle was calculated from:  $\cos \varphi = d_{(100)}/h$ .

Molecule	T (°C)	$2\theta$ (°)	$l$ (nm)	$^aL$ (nm)	$2\theta$ (°)	$d_{(100)}$ (nm)	$^bh$ (nm)	Tilt angle (°)
<b>5BEgly-H (17)</b>	25	2.53	3.49	3.24	4.13	2.14	2.80	40
<b>7BEgly-H (20)</b>	25	2.0	4.41	4.68	3.78	2.33		33
	50	2.02	4.37	4.68	3.78	2.33		33
	70	2.05	4.30	4.68	3.80	2.32	2.80	34
	85	-	-	4.68	3.80	2.32		34
<b>I-nBEgly (13)</b>	25	-	-	-	4.41	2.00	2.80	45

<sup>a</sup>Theoretical length of the phenyleneethynylene backbone

<sup>b</sup>Theoretical molecular length on its more extended conformation and in a bilayer assembling

result is in disparity with what has been reported for short oligo(phenyleneethynylene)s, where the dihedral angle is almost zero. For instance, Li et al.<sup>13b</sup> reported a dihedral angle of 2.35° for a 2,5-bis(methoxy)phenylene-ethynylene dimer, while James et al. found that a non-substituted trimer is totally planar (with just one possible minimum conformation); in addition, a trimer bearing a 2,5-bis(hexyloxy) side chain in the central phenyleneethynylene presents the lowest energetic conformation, where both the side chains and phenyls are in the same plane. Nevertheless, these authors demonstrated that the energy barrier for phenyl rotations is very low giving rise to energetically close-twisted conformations<sup>12</sup>.

In our case, we relate the dihedral angle of **3BEgly-H** to the fact that it is a benzoate-ethynylene type oligomer and that the glycol side chains indeed have an influence. In contrast, the **5BEgly-H** shows a practically planar structure in its lowest energy geometry, with dihedral angles of 6°, 16°, 1° and 20° as is shown in Fig. 4b.

**Excitation energies.** Starting from the previous minimum conformations found at the AM1 level, the excitation energies and their corresponding oscillator strength ( $f$ ) for the first four singlet and triplet states were calculated and the values summarized in Table 3. The predicted maximum of the absorption is red-shifted with respect to the experimental maximum; this difference (with respect to the transition with largest oscillator strength) is of 44 nm for **3BEgly-H** and of 76 nm for **5BEgly-H**. This result is expected since TDDFT usually sub-estimates the eigenvalues<sup>7</sup>. The presence at 378 nm of a quasi-degenerate triplet state for **3BEgly-H** suggests that the non-radiative relaxation pathway is favorable for this oligomer. However, **5BEgly-H** also presents a triplet state at 458 nm, even closer to the singlet one than in **3BEgly-H**, which should suggest an appreciable contribution of intersystem crossing competition with the fluorescence. As this result is contrary to the experimental values, where the quantum yield for this oligomer is very high and higher than the trimer, we consider that this conformation is not the more accurate for the pentamer. In this respect, it is to be pointed out that the optimization process is carried out in vacuum, while experimentally; the presence of the solvent may affect the chain interactions and consequently the dihedral angles between benzoates. Thus, under this hypothesis, we proceeded to vary the phenyl dihedral angles, i.e., [90°,90°], [90°,45°] and [45°,45°] for **3BEgly-H** and of [45°, 45°, 0°, 10°] [60°, 45°, 45, 60] and [60°, 60°, 90°, 60°] for **5BEgly-H**. Constrained

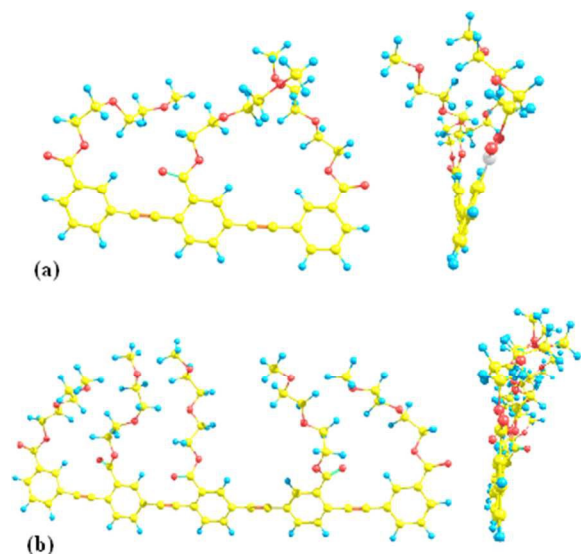


**Fig. 4** Front and side view of the lowest energetic conformation of: (a) trimer **3BEgly-H** ( $E = -351.87$  Kcal/mol) and (b) pentamer **5BEgly-H** ( $E = -543.29$  Kcal/mol), obtained from AM1 calculations.

structures were re-optimized by TDDFT and the values found are summarized in Tables 1s and 2s. It can be noted that geometries that better reproduce the experimental absorption maxima correspond to those shown in Fig. 5, where the dihedral angles between the two neighbor benzoates are of 90° and 45° for the trimer, while for the pentamer, are 60°, 60°, 90° and 60°.

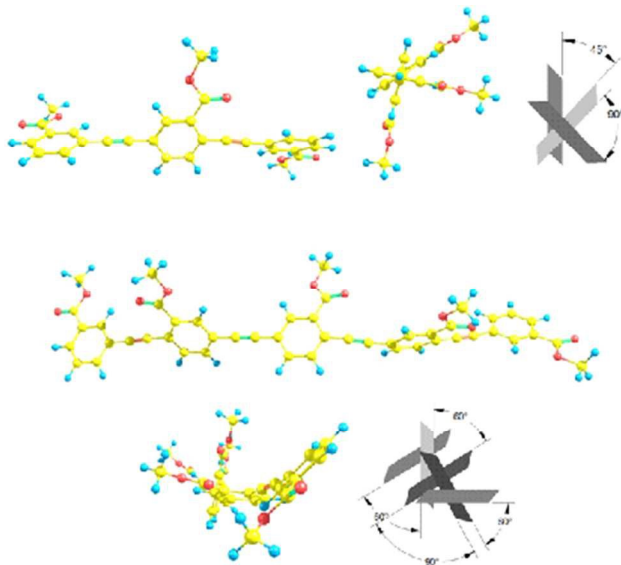


**Fig. 5** Geometry of (top) **3BEgly-H** with dihedral angles between the benzoate planes of 90° and 45°, (bottom) **5BEgly-H** with dihedral angles between the benzoate planes of 60°, 60°, 90° and 60°, respectively.

The corresponding excitation energies for the first four singlet and triplet excited states are also reported in Table 4. Notice that the absorption peaks match well with the experimental ones with a red-shift of 11 and 15 nm for the **3BEgly-H** and **5BEgly-H**, respectively. Further calculations on the optimized geometry of **3BEgly-H**, including the diethylene glycol methyl ether side chains by the TD-B3LYP/6-311G\*\* basis, gave no differences, thus validating the hypothesis that the glycol side chains do not affect the electronic transitions. From data of Table 4, it is also noteworthy that the energy difference between the first allowed optical transitions and the nearest triplet state is 0.02 eV for **3BEgly-H** and 0.16 eV for **5BEgly-H**. This result is consistent with the experimental observation that the pentamer is more fluorescent than the trimer. In fact, assuming that these channels are active as non-radiative pathways, the practical degeneracy of singlet-triplet state in the case of the **3BEgly-H** suggests that the probability of an intersystem crossing is more evident for this oligomer than for **5BEgly-H**, which has the higher quantum yield.

### Thermal and structural properties

The thermal behaviour of the hydrogen terminated oligomer series was examined by differential scanning calorimetry (DSC), polarized-light optical microscopy (POM) and small and wide angle X-ray scattering (SWAXS). The thermograms of the series are shown in Fig. 6. It is worth mentioning that

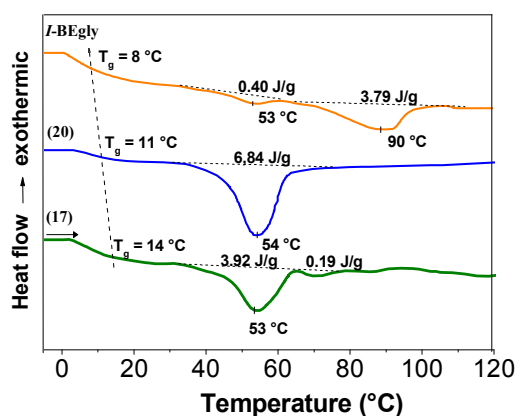


**Fig. 6** Thermograms of the first heating of **5BEgly-H** (17), **7BEgly-H** (20) and of *I*-nBEgly (13). The heating was performed at a scanning rate of 10 °C/min under nitrogen.

these three macromolecules exhibited transitions only during the first heating, while in the crystallization or in the second heating cycles, no any appreciable transition was observed; **3BEgly-H** is highly viscous, thus isotropic. As can be seen in Fig. 6, **5BEgly-H** and **7BEgly-H** show a similar broad endothermic peak from 32 °C up to 75 °C with rather low melting enthalpies. However that of **7BEgly-H** ( $\Delta H_m = 6.84$  J/g) is relatively higher than that of **5BEgly-H** ( $\Delta H_m = 4.11$  J/g). These broad endotherms are due to the transition between the liquid crystalline phase of the layered type and the isotropic melt of both oligomers, which was also corroborated by POM. The low fusion enthalpy of the polymer, 4.2 J/g, is attributed to the lower molecular fractions, because no fusion was observed by POM. Although, the development of any known texture reported in the literature was not observed, the materials are strongly birefringent and pasty, suggesting the existence of mesomorphism. An important feature of these oligomers is the development of a glass transition phase ( $T_g$ ), whose temperature decreases as the length of the oligomer increases, being of 14 °C, 11 °C and of 8 °C for the pentamer, heptamer and polymer, respectively. It seems that: i) the oxygen of the (diethylene glycol methyl ether) chains produces enough free rotation to generate an increase of the molar volume, phenomena that we have not observed before in other similar (cholesteryl)<sup>7</sup> or (11-undecano)<sup>3a</sup> or (dodecane) benzoateethynylene<sup>17</sup> oligomers, and that is facilitated because the oxyethylene chains are methyl end capped, and ii) in agreement with Meyer<sup>18</sup> on poly(p-phenylenes) substituted with oxyethylene side chains, that the main chain order, due to the  $\pi$ - $\pi$  interaction, seems to facilitate the occurrence of side chain crystallization.

The scattering patterns of **5BEgly-H**, **7BEgly-H** and *I*-nBEgly as powders in capillaries at room temperature are presented in Fig. 7a; all of the calculated structural parameters are summarized in Table 5. A single molecule of these materials, in its more extended conformation, gives a theoretical distance of 1.48 nm (ESI), Fig. 7b, while that obtained by SWAXS is of  $d_{(100)}$  2.13 and 2.33 nm for **5BEgly-H** and **7BEgly-H**, respectively, Fig. 7a. This means that the molecules self-



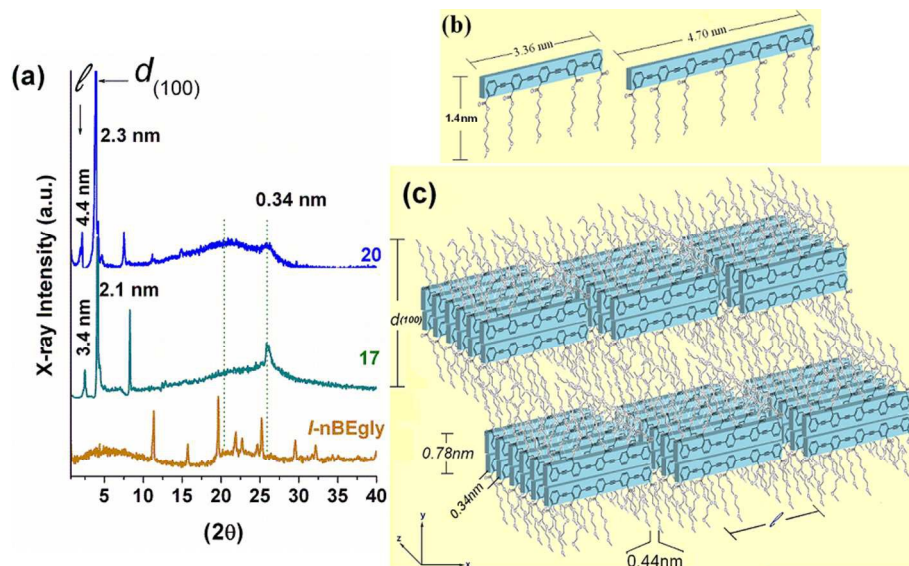


**Fig.7** (a) Room temperature X-ray scattering patterns of **5BEgly-H** (17), **7BEgly-H** (20) and of **I-nBEgly** (13). (b) Theoretical lengths of the benzoateethynylene backbone and of their more extended conformation for **5BEgly-H** (17) and **7BEgly-H** (20). (c) General sketch representing the possible molecular order of the materials deduced from X-ray patterns. The different molecular net parameters such as  $d_{(100)}$ ,  $2\theta$ ,  $\angle$ , and tilt angle of the side chains are collected in Table 3.

assemble in a bilayer conformation, such as we have observed for other (alkyl)benzoateethynylene macromolecules<sup>7,3,17</sup>, where the side chains are oriented in an opposite sense in a back-to-back comb like “style” as is depicted in Fig. 7c. Another feature that supports this assembly is the diffraction peak that appears at a  $2\theta$  of  $11.29^\circ$  ( $d$  0.78 nm), which corresponds to the distance of two phenyls. This was also identified by HRTEM analysis of a film of a (cholesterly) benzoateethynylene oligomer by a beam incidence parallel to the surface ( $90^\circ$ ), while by perpendicular incidence, we observed a periodicity of 0.33 nm assigned to the distance between conjugated chains<sup>7</sup>. However, it can be seen that the theoretical distance  $h$  of 2.96 nm does not match the experimentally found distances (along the  $y$  direction and that give rise to the plane  $d_{(100)}$ ) of 2.14, 2.33 and 2.0 nm for **5BEgly-H**, **7BEgly-H** and **I-nBEgly**, respectively, meaning that the diethylene glycol methyl ether chains are tilted 40, 33 and  $45^\circ$ , respectively. The four high order reflections at  $2\theta$  of 4.14, 8.29, 12.56° and  $15.40^\circ$  for **5BEgly-H** and of 3.78, 7.38, 11.29 and  $14.72^\circ$  for **7BEgly-H**, with ratios of ca. 1:2:3:4, are indicative of lamellar systems, therefore the signatures of Smectic C mesophases could be considered for these two oligomers, while that of Nematic type for the polymer. The latter actually shows a series of very thin diffraction peaks that are indicative of aggregates. The side chains give rise to a very diffuse halo with an average distance of 0.44 nm, meaning that the chains are amorphous in all of the materials. It can be seen that there is a relative long range order of the benzoateethynylene backbones in the  $z$  direction, which is supported by the diffused halo that appears in the diffractograms at  $2\theta$  of  $25.8^\circ$  ( $d$  0.34 nm) and that is related to

the  $\pi$ - $\pi$  interaction, such as that observed for the (11-undecanol) benzoateethynylenes oligomers<sup>3a</sup>. In general, we had found that these materials have a tendency to pack in blocks of molecules resembling bricks that are randomly oriented and that have been named as “Sanidic” LC’s<sup>7,8</sup> as a general term to classify this mesomorphism. Additionally, temperature dependent X-ray scattering carried out on **7BEgly-H** showed no change of the Bragg peak or the appearance of another mesophase as a function of temperature, Fig. 8. For the **5BEgly-H** see ESI. We point out that we have never observed in other similar series the diffraction peaks exhibited by **5BEgly-H** and **7BEgly-H** at  $2\theta$  of 2.53 and  $2.0^\circ$ , with corresponding distances of 3.49 and 4.41 nm and that match well with the theoretical length of their benzoateethynylene backbone (along the  $x$  direction) of 3.24 and 4.68 nm, respectively, Fig. 7b. On the basis of these results, it seems that these bricks of molecules present a certain order in the  $x$ ,  $y$  and  $z$  directions, which is not commonly observed in phenyleneethynylene macromolecules.

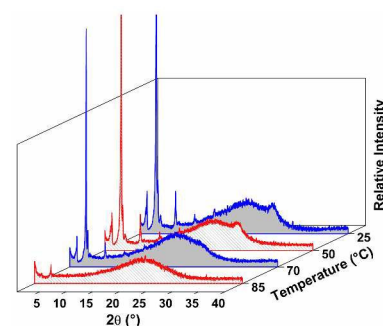


**Fig. 8.** Temperature dependent X-ray scattering patterns of **7BEgly-H** (20).

Cast films of **5BEgly-H**, **7BEgly-H** and **I-nBEgly** deposited on Lacey-carbon grids were analyzed in planar view by HRTEM. In general, it was found that the main chain layers of all domains in the film are preferentially oriented perpendicular to the film surface, because i) a periodicity of 0.35 nm was found as is observed in Fig. 9a-c, and ii) because the corresponding selected area electron diffraction analyses (SAED), Fig. 9c-f, show a reflection at  $d = 0.35$  nm. We note that the SAED of **5BEgly-H** shows very well-defined spots such as would correspond to a single crystal, however, from the X-ray analysis; we deduced that this oligomer exhibits an hexatic mesophase with a columnar arrangement, which could be visualized as the sketch in Fig. 9d. In Fig. 9b, we schematize the supramolecular model of organization deduced by HRTEM analysis, where plans consist of bilayers of benzoateethynylene aligned in perpendicular fashion to the film surface and separated by 0.35 nm; a distance that gives evidence of the strong  $\pi$ - $\pi$  interactions that govern these materials.

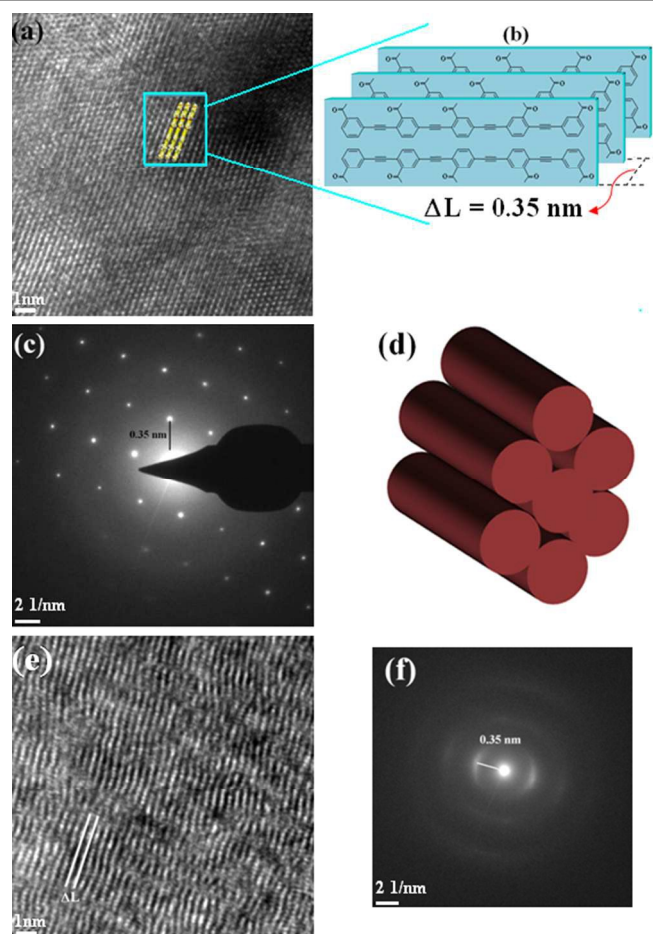


**Fig. 9** (a) High Resolution Transmission Microscopy (HRTEM) image of a film of **7BEgly-H** (**20**) deposited on Lacey-carbon grid. (b) The periodicity ( $\Delta L$ ) of 0.35 nm corresponds to the distance between planes of conjugated molecules as sketched at the right. (c) Selected area electron diffraction patterns (SAED) of a film of **5BEgly-H** (**17**), and (d) the possible hexatic columnar arrangement of the molecules deduced by SWAXS. (e) HRTEM image of **I-nBEgly** (**13**), (f) the calculated periodicity of  $\Delta L = 0.35$  nm is also confirmed by SAED at right.

## CONCLUSIONS

In conclusion, a family of benzoateethynylene oligomers bearing highly polar diethylene glycol methyl ether as side chains was selectively synthesized by applying two sets of reactions at each cycle: a Sonogashira cross-coupling and a iodination by the bi-directional iterative divergent-convergent approach giving rise to odd number oligomers, i.e., a trimer, pentamer and heptamer. A bathochromic shift was observed when passing from the trimer, to the pentamer, heptamer, and then to the polymer, as a result of the increase in the  $\pi$ -electron delocalization of the conjugated backbone. The diethylene glycol methyl ether side chains strongly enhance the fluorescence quantum yield with respect to other cholesteryl or 11-undecanol side chains. Actually, the pentamer is the most fluorescent oligomer with a quantum yield in solution of  $\phi(\%) = 70 - 97$  and a fluorescence lifetime of 0.25 – 0.43 ns, depending on the solvent and making this oligomer suitable for optoelectronic devices. Both HRTEM and X-ray analyses support the concept that a strong  $\pi$ - $\pi$  interaction governs in all of the macromolecules series, giving rise to their supramolecular self-assembling in bilayers in a back-to-back superposed comb style, and forming blocks of aggregates separated by 0.35 nm between conjugated chains. The general term to classify the mesomorphic behavior of these materials is Sanidic LCs, which is consistent with their molecular shape assembly, reassembling bricks or board-like structures.

## ACKNOWLEDGEMENTS

This work was financially supported by CONACYT through the projects 98513-R and 232753 Laboratorio Nacional de Materiales Grafénicos. Authors also thank Guadalupe Mendez, Gabriela Padron, Teresa Rodríguez and Silvia Torres for their technical assistance.

## NOTES AND REFERENCES

<sup>a</sup>Centro de Investigación en Química Aplicada (CIQA), Blvd. Enrique Reyna 140, 25294, Saltillo, México. Tel: 00528444389830, Fax: 00528444389839, e-mail: eduardo.arias@ciqa.edu.mx

<sup>b</sup>Dipartimento di Chimica e Chimica Industriale, Università di Genova, Via Dodecaneso 31, 16146 Genoa, Italy

Electronic Supplementary Information (ESI) available: [Scheme 1S, experimental procedures, theoretical calculations, <sup>1</sup>H, APT, <sup>13</sup>C NMR spectra, SAXs diffraction patterns of **17** at different temperatures, photophysical properties in solution of oligomers are given]. See DOI: 10.1039/b000000x/

- 1 T. McQuade, A. E. Pullen, T. M. Swager, *Chem. Rev.*, 2000, **100**, 2537-2574.
- 2 E. Vazquez, A. Esquivel, I. Moggio, E. Arias, J. Romero, H. Barrientos, J. Roman, M. de L. Reyes, *Mater. Sci. Eng. C*, 2007, **27**, 787-793.
- 3 (a) E. Arias, J.C. Arnault, D. Guillon, T. Maillou, J. Le Moigne, B. Geffroy, J.M. Nunzi, *Langmuir*, 2000, **16**, 4309-4318. (b) E. Arias, J.

- Le Moigne, T. Maillou, D. Guillon, I. Moggio, B. Geffroy, *Macromolecules*, 2003, **36**, 3570-3579.
- 4 I.-B. Kim, H. Shin, A. J. Garcia, U. H.F. Bunz, *Bioconjugated Chem.*, 2007, **18**, 815-820.
- 5 R. L. Phillips, I.-B. Kim, B. E. Carson, B. Tidbeck, Y. Bai, T. L. Lowary, L. M. Tolbert, U. H. F. Bunz, *Macromolecules*, 2008, **41** (20), 7316-7320.
- 6 G. Castruita, E. Arias, I. Moggio, F. Pérez, D. Medellín, R. Torres, R. Ziolo, A. Olivas, E. Giorgetti, M. Muniz-Miranda, *J. Mol. Struct.*, 2009, **936**, 177-186.
- 7 G. Castruita, V. García, E. Arias, I. Moggio, R. Ziolo, A. Ponce, V. González, J.E. Haley, J.L. Flikkema, *J. Mater. Chem.*, 2012, **22**, 3770-3780.
- 8 (a) L. Kloppenburg, D. Jones, J.B. Claridge, H-C. Loye, U.H.F. Bunz, *Macromolecules*, 1999, **32**, 4460-4463. (b) J.N. Wilson, P.M. Windscheif, U. Evans, M.L. Myrick, U.H.F. Bunz, *Macromolecules*, 2002, **35**, 8681-8683.
- 9 A.T.R. Williams, S.A. Winfield, J.N. Miller, *Analyst*, 1983, **108**, 1067-107.
- 10 S. A. El-Daly, S. A. El-Azim, F. M. Elmekawey, B. Y. Elbaradei, S. A. Shama, A. M. Asiri, *International Journal of Photoenergy*, 2012, **2012**, 1-10.
- 11 H. Barrientos, E. Arias, I. Moggio, J. Romero, O. Rodríguez, E. Giorgetti, T. Del Rosso, *Synthetic Metals*, 2004, **147**, 267-270.
- 12 P. V. James, P. K. Sudeep, C. H. Suresh, K. G. Thomas, *J. Phys. Chem. A*, 2006, **110**, 4329-4337.
- 13 a) L.T. Liu, D. Yaron, M.I. Sluch, M.A. Berg, *J. Phys. Chem. B*, 2006, **110**, 18844. b) N. Li, K. Jia, S. Wang, A. Xia, *J. Phys. Chem. A.*, 2007, **111**, 9393. c) Y. Matsunaga, K. Takeshi, T. Akasaka, A.R. Ramesh, P.V. James, K.G. Thomas, P.V. Kamat, *J. Phys. Chem. B*, 2008, **112**, 14539.
- 14 I. B. Berlman, *Handbook of Fluorescence Spectra of Aromatic Molecules*, 2nd ed., Academic Press: London, New York, 1971.
- 15 J.R. Lakowicz, *Principles of fluorescence spectroscopy*, Kluwer Academia/Plenum Publishers, 1999.
- 16 J.-S. K. Yu, W.-C. Chen, C.-H. Yu, *J. Phys. Chem. A*, 2003, **107**, 4268-4275.
- 17 P. Wautelet, M. Moroni, L. Oswald, J. Le Moigne, A. Pham, J.Y. Bigot, *Macromolecules*, 1996, **29**, 446-455.
- 18 (a) U. Lauter, W.H. Meyer, G. Wegner, *Macromolecules*, 1997, **30**, 2092. (b) U. Lauter, W.H. Meyer, V. Enkelmann, G. Wegner, *Macromol. Chem. Phys.*, 1998, **199**, 2129.